JOURNAL OF MATERIALS SCIENCE 26 (1991) 6491–6495

Microstructure and mechanical properties of cordierite ceramics toughened by monoclinic ZrO_2

YOUNG-JEI OH, TAE-SUNG OH, HYUNG-JIM JUNG
Division of Ceramics, Korea Institute of Science and Technology, PO Box 131, Cheongryang, Seoul, Korea

The effects of m-ZrO_2 addition on the mechanical behaviour of the cordierite ceramics were studied. Below 10 vol% of m-ZrO_2 content, zircon ($ZrSiO_4$) was formed as a second phase at the expense of all m-ZrO_2 due to the reaction between ZrO_2 and silica in the cordierite. The sintered density was improved with ZrO_2 addition through glass phase formation along grain boundaries, and maximum sinterability was obtained at 4.6 vol% m-ZrO_2. When sintered at 1300 °C for 4 h, the flexural strength at 4.6 vol% ZrO_2 was 190 MPa, compared with 55 MPa for the pure cordierite. Fracture toughness was gradually enhanced from 1.75 MPa $m^{1/2}$ to 2.4 MPa $m^{1/2}$ with m-ZrO_2 addition up to 10 vol%, which could be explained partly by thermal expansion mismatch between cordierite and the second-phase $ZrSiO_4$ and partly by crack deflection at the cordierite–$ZrSiO_4$ interfaces.

1. Introduction

Cordierite ($2MgO \cdot 2Al_2O_3 \cdot 5SiO_2$) has several advantageous properties, such as a low dielectric constant of about 4.6, low thermal expansion coefficient ($2.3 \times 10^{-6}\,°C^{-1}$) and low fabrication temperature, to be used as an electronic packaging substrate with Cu interconnections [1] or thermal shock-resistant material [2, 3]. However, mechanical failure, due to its low fracture toughness, during subsequent processing such as pin brazing would cause serious reliability problems for its application.

Ceramics dispersed with ZrO_2 as a second phase have been extensively investigated to improve the mechanical properties of alumina, mullite, Si_3N_4, dental porcelain and glass–ceramics [4–10]. Recently, toughening of cordierite has been reported with ZrO_2 dispersion higher than 20 vol% [11, 12]. With such high ZrO_2 content, however, the dielectric constant, which is the most advantageous property of the cordierite as an electronic packaging substrate, would become high, resulting in an increase of the signal-propagation delay in the packaging structure.

In the present study, therefore, cordierite was fabricated with a dispersion of unstabilized ZrO_2 (m-ZrO_2) up to 10 vol%, and characteristics of the sintered composites, such as sinterability and mechanical properties, were evaluated with the emphasis on the examination of the toughening mechanisms. Below 10 vol% of m-ZrO_2 content, all ZrO_2 particles were consumed to form a $ZrSiO_4$ phase by reaction with the cordierite, which affected the sintering behaviour of the cordierite. Without any ZrO_2 particles remaining in the cordierite matrix, toughening of this material was thus explained partly by the thermal expansion mismatch stresses between cordierite and $ZrSiO_4$, and partly by crack deflection around $ZrSiO_4$ particles.

2. Experimental procedure

The equivalent particle size of commercial cordierite powder was 18 μm, and the surface area of m-ZrO_2 was $12\,m^2\,g^{-1}$. Powders were mixed in the desired ratio, as shown in Table I, in a high-density alumina ball mill with water and then dried. The batches were isostatically pressed under 140 MPa to fabricate test bars (5 mm × 7 mm × 30 mm) and then sintered at different temperatures from 1200 to 1350 °C for 4 h in air. The heating and cooling rates were $\pm 10\,°C\,min^{-1}$. Bulk density of the sintered bodies was measured using the Archimedes technique. Flexural strength of the test bars was determined in three-point bending with a span of 20 mm. The Vickers microhardness and fracture toughness were determined by the indentation method [13]. The phases and microstructure of the composites were characterized using X-ray diffraction (XRD), scanning electron microscopy (SEM) and transmission electron microscopy (TEM).

3. Results and discussion

3.1. Sintering behaviour of cordierite with m-ZrO_2 content

As shown in Fig. 1, the bulk density of the cordierite–m-ZrO_2 composite, fired at 1300 °C for 4 h, increased with the m-ZrO_2 content. Contrary to the sintering behaviour of Al_2O_3–ZrO_2 composite where densification of Al_2O_3 was retarded with ZrO_2 addition [14], the sinterability of the cordierite was enhanced and the maximum sinterability was obtained at 4.6 vol% m-ZrO_2.

0022–2461/91 $03.00 + .12

TABLE I Chemical composition of the specimens

Component	Specimen symbol					
	Co	CZ_2	CZ_5	CZ_{10}	CZ_{15}	CZ_{20}
Cordierite	100	99.1	97.7	95.4	92.8	90.1
m-ZrO_2	–	0.9	2.3	4.6	7.2	9.9

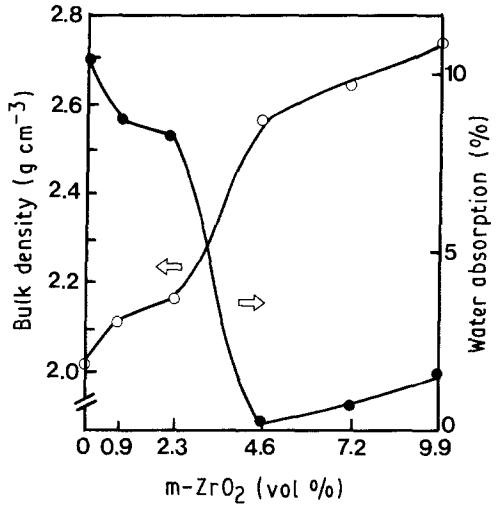

Figure 1 (○) Bulk density and (●) water absorption of cordierite specimens as a function of m-ZrO_2 content.

Although it has been reported that a second phase was not formed by the reaction between ZrO_2 and Al_2O_3 [14], zircon ($ZrSiO_4$) was produced in all compositions examined in this study due to the reaction between ZrO_2 and free silica from the cordierite. Thus the residual glass phase remaining along the grain boundaries, after the formation of $ZrSiO_4$, as observed in Fig. 2, may enhance the sinterability of the cordierite through liquid-phase sintering. However, a remarkable increase of the $ZrSiO_4$ phase in the composites above 4.6 vol % m-ZrO_2, as illustrated by SEM (Fig. 3), may hinder the densification, resulting in decreased sinterability. Fig. 3 shows the homogeneous dispersion of $ZrSiO_4$ phase in the cordierite matrix. The fraction of pores in the composites decreased with ZrO_2 content up to 4.6 vol % m-ZrO_2, but became higher with further addition of ZrO_2. This agrees well with the water absorption behaviour shown in Fig. 1.

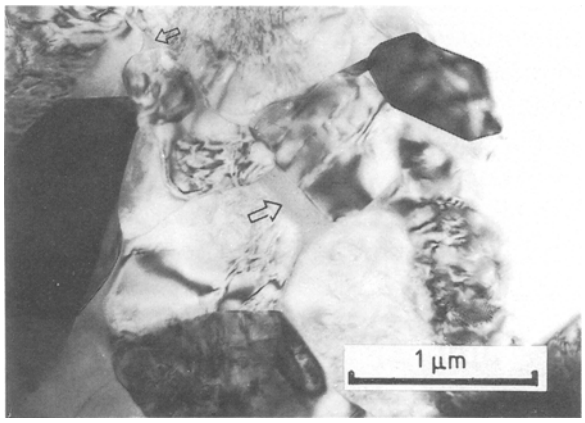

Figure 2 Transmission electron micrograph of cordierite composite with 4.6 vol % m-ZrO_2 addition. The arrows show glassy phase around the grain boundary.

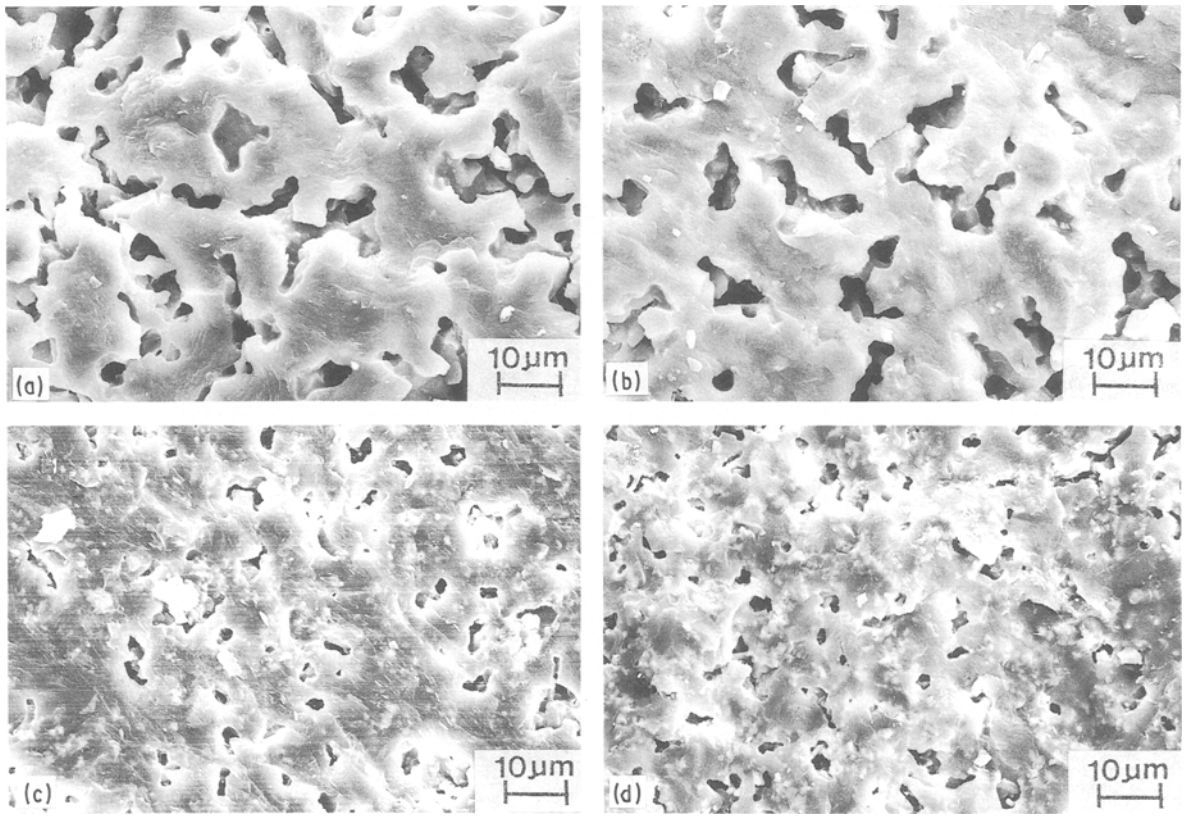

Figure 3 Fracture surfaces of cordierite containing (a) 0, (b) 0.9, (c) 4.6 and (d) 9.9 vol % m-ZrO_2. All samples were sintered at 1300 °C for 4 h.

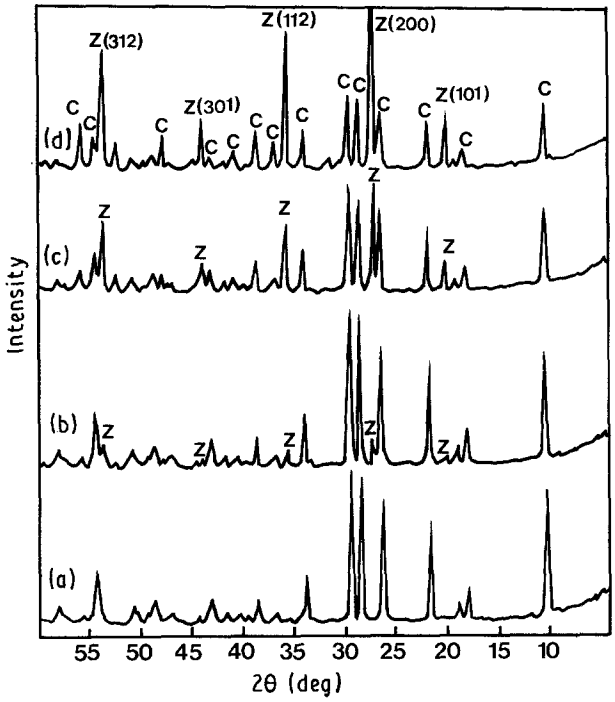

Figure 4 X-ray diffraction patterns of the as-sintered cordierite–ZrO_2 composites: (a) Co, (b) CZ_2, (c) CZ_{10}, (d) CZ_{20}, (C = cordierite, z = zircon).

As shown in Fig. 4, XRD patterns of cordierite containing m-ZrO_2 indicate that the amount of $ZrSiO_4$ increased with increasing m-ZrO_2 content, and ZrO_2 phase could not be detected in any of the compositions examined in this study. A similar trend was also observed with t-ZrO_2 addition. However, the effect of the firing temperature on the formation of $ZrSiO_4$ second phase was found to be insignificant. The formation of $ZrSiO_4$ has been observed during crystallization of cordierite–ZrO_2 glass–ceramic [9] and sintering of cordierite–ZrO_2 powder mixture [12] at temperatures above 1250 °C. With the solubility of ZrO_2 in the cordierite about 5 vol % [15], unreacted ZrO_2 particles were detected in the cordierite matrix with an intergranular glass phase at ZrO_2 contents above 20 vol % [11, 12]. However, below 10 vol % of ZrO_2 content, particularly with the fine powders of surface area of 12 $m^2 g^{-1}$ used in this study, ZrO_2 may fully react with the cordierite, forming $ZrSiO_4$ second phase without any ZrO_2 particles remaining in the sintered body (Fig. 4). Thus the sintering behaviour of the cordierite with ZrO_2 addition is closely related to the formation of $ZrSiO_4$ and intergranular glass phase.

3.2. Mechanical properties of cordierite–ZrO_2 composites

Fig. 5a shows the flexural strength of cordierite, as a function of m-ZrO_2 content, when sintered at 1300 °C for 4 h. The maximum flexural strength of 190 MPa, which was about four times higher than the 55 MPa of pure cordierite, was obtained at 4.6 vol % m-ZrO_2 where the maximum sinterability was obtained (Fig. 1). The effect of sintering temperature on the flexural strength of composites containing 4.6 vol % m-ZrO_2 is summarized in Fig. 5b. Whereas the flexural strength of pure cordierite increased with increasing firing temperature due to densification, the strength of cordierite–ZrO_2 increased with sintering temperature up to 1300 °C and then dropped due to the formation of excess glass phase along the grain boundaries (Fig. 2).

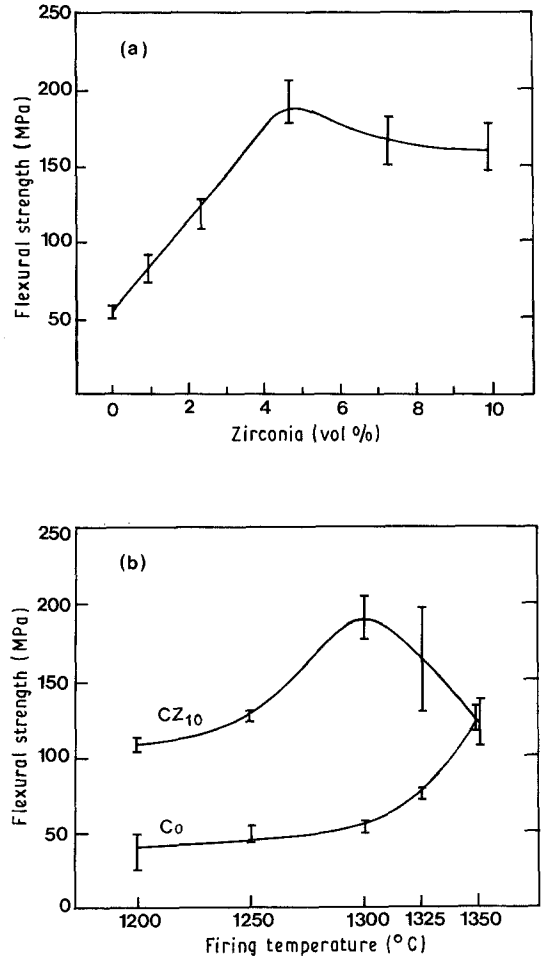

Figure 5 Flexural strength of cordierite as a function of (a) m-ZrO_2 content, when sintered at 1300 °C for 4 h, and (b) sintering temperature at 4.6 vol % m-ZrO_2.

The fracture toughness of the cordierite, shown in Fig. 6, was enhanced with the addition of ZrO_2. Generally, toughening of ceramics with ZrO_2 can be achieved through microcracking with m-ZrO_2 dispersion and martensitic transformation from tetragonal to monoclinic phase with t-ZrO_2 [4–10]. Such a concept was also applied to the toughness improvement of cordierite with ZrO_2 dispersion higher than 20 vol % [11, 12]. Below 10 vol % of ZrO_2 content, however, there were no ZrO_2 particles remaining in the cordierite due to the full reaction between ZrO_2 and cordierite to form $ZrSiO_4$ phase, as confirmed by the XRD analysis (Fig. 4). The toughening mechanism will therefore be quite different from that in conventional ZrO_2-toughened ceramics, and this toughening may not depend on the crystal structure of the dispersed ZrO_2 (tetragonal or monoclinic). Indeed, preliminary XRD examinations of cordierite containing t-ZrO_2 up to 10 vol % show the formation of $ZrSiO_4$ second phase with the consumption of all t-ZrO_2 particles.

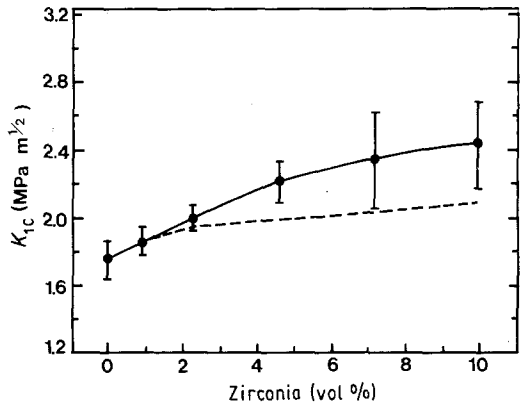

Figure 6 Fracture toughness of cordierite, as a function of m-ZrO_2, fired at 1300 °C for 4 h: (●) measured, (– – –) estimated from thermal mismatch.

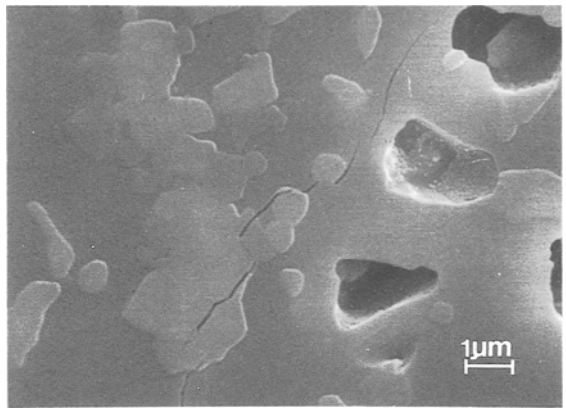

Figure 7 Scanning electron micrograph of cordierite–$ZrSiO_4$ composites showing crack-propagation behaviour at 4.6 vol % m-ZrO_2 addition.

Supposing that all ZrO_2 has reacted to $ZrSiO_4$, the residual compressive stress in the cordierite matrix and tensile stress in the $ZrSiO_4$ second phase will be developed during cooling from the firing temperature due to the lower thermal expansion coefficient of the cordierite ($2.3 \times 10^{-6}\,°C^{-1}$) compared to the value for $ZrSiO_4$ ($4.8 \times 10^{-6}\,°C^{-1}$).

Neglecting partial relaxation of the residual stresses due to viscous deformation of the intergranular glass phase formed during reaction between cordierite and ZrO_2 [12], the hydrostatic stress, σ_z, imposed in $ZrSiO_4$ particles during cooling from fabrication temperature, can be calculated as [16, 17]

$$\sigma_z = \frac{2\Delta\alpha\Delta T E_c E_z}{(1 + \nu_c)E_z + 2(1 - 2\nu_z)E_c} \quad (1)$$

where $\Delta\alpha$ is the difference of the thermal expansion coefficients and ΔT is the cooling range from the sintering temperature; E_c, ν_c and E_z, ν_z are the Young's modulus and Poisson's ratio of cordierite and $ZrSiO_4$ phase, respectively. With $\Delta\alpha = 2.5 \times 10^{-6}\,°C^{-1}$, $E_c = 120$ GPa, $E_z = 230$ GPa, $\nu_c = 0.25$ and $\nu_z = 0.3$, the magnitude of the residual tensile stress imposed on $ZrSiO_4$ particles is 280 MPa, which is much lower than 1480 MPa which would be developed in the m-ZrO_2 phase if $ZrSiO_4$ were not formed. The residual compressive stresses on the cordierite matrix, then, can be calculated from the notion that macrostresses in the cordierite–$ZrSiO_4$ composites should be zero, that is [12]

$$\sigma_c f_c + \sigma_z f_z = 0 \quad (2)$$

where f_c and f_z are the volume fractions of cordierite and $ZrSiO_4$, respectively, which could be calculated from the volume fraction of m-ZrO_2 addition.

The crack will then propagate through alternate zones of uniform tension and compression with an oscillating stress intensity factor expressed as [18]

$$K_c = K_m + 2\sigma_c\left(\frac{2D_z}{\pi}\right)^{1/2} \quad \text{(compressive zone)} \quad (3)$$

$$K_c = K_p - 2\sigma_z\left(\frac{2D_z}{\pi}\right)^{1/2} \quad \text{(tensile zone)} \quad (4)$$

where K_m and K_p are the critical stress intensity factors for the matrix and the $ZrSiO_4$ particles, respectively, and D_z is the zone length which can be estimated to be of the order of the interparticle spacing [12, 19]. The fracture toughness of this type of composite is determined by the maximum value of the oscillating stress intensity factor [20], and is plotted in Fig. 6 as a function of ZrO_2 content. However, comparisons with measured fracture toughness indicate that residual compressive stress in the cordierite could only partially explain the toughness increment, especially at high ZrO_2 content.

Observations of indentation cracks (Fig. 7) indicate that cracks propagated around the $ZrSiO_4$ phase with more deflection at higher $ZrSiO_4$ content. Thus the crack surface area was increased with an increase in m-ZrO_2 addition, as observed in the ZnO–ZrO_2 system [21]. Assuming that $ZrSiO_4$ particles are of spherical shape and uniformly distributed in the matrix, the toughness increment due to crack deflection, ΔK, can be estimated as [22]

$$\Delta K = (1 + 0.87 f_z)^{1/2} K_m - K_m \quad (5)$$

where f_z is the volume fraction of $ZrSiO_4$ phase and K_m is the toughness of the cordierite matrix. This extrinsic toughening through crack deflection may explain the discrepancy between the measured fracture toughness and values estimated from thermal mismatch stresses. Thus the toughening of the cordierite with m-ZrO_2 dispersion is considered to derive from the thermal expansion mismatch stresses between cordierite and $ZrSiO_4$ second phase, and the crack deflection process around $ZrSiO_4$ particles.

4. Conclusions

Based on the study of the toughening of cordierite with m-ZrO_2 dispersion up to 10 vol %, the following conclusions can be drawn:

1. The sintering of cordierite was enhanced by m-ZrO_2 addition through glass phase formation along grain boundaries, and maximum sinterability was found at 4.6 vol % m-ZrO_2. Below 10 vol %, it was found that all m-ZrO_2 has reacted with cordierite

to form $ZrSiO_4$ second phase. With ZrO_2 addition above 4.6 vol %, the remarkable increase of $ZrSiO_4$ phase may hinder the densification.

2. The maximum flexural strength at 4.6 vol % m-ZrO_2, 190 MPa, was about four times higher than the 55 MPa of pure cordierite. The strength of cordierite at 4.6 vol % m-ZrO_2 increased with increasing sintering temperature up to 1300 °C due to the enhanced densification. With further increasing sintering temperature, however, the strength was reduced due to the formation of excess glass phase along the grain boundaries.

3. The fracture toughness of cordierite was increased from 1.75 to 2.4 MPa $m^{1/2}$ with addition of m-ZrO_2 up to 10 vol %. This toughening was partly attributed to the residual compressive stresses imposed on the cordierite due to thermal expansion mismatch between cordierite and $ZrSiO_4$ second phase, and partly to crack deflection around $ZrSiO_4$ particles especially at higher ZrO_2 content.

Acknowledgements

The authors thank Drs S. W. Park and Y. B. Shon for helpful discussions.

References

1. R. R. TUMMALA, in "Microelectronics Packaging Handbook", edited by R. R. Tummala and E. J. Rymaszewski (Van Nostrand Reinhold, New York, 1989) p. 500.
2. P. PREDECKI, J. HAAS, J. FABER and R. L. HITTERMAN, *J. Amer. Ceram. Soc.* **70** (1987) 175.
3. H. IKAWA, T. OTAGIRI, O. IMAI, M. SUZUKI, K. URABE and S. UDAGAWA, *ibid.* **69** (1986) 492.
4. N. CLAUSSEN, *ibid.* **59** (1976) 49.
5. F. F. LANGE, *J. Mater. Sci.* **17** (1982) 247.
6. N. CLAUSSEN and J. JAHN, *J. Amer. Ceram. Soc.* **63** (1980) 228.
7. N. CLAUSSEN, R. WAGNER, L. J. GAUCKLER and G. PETZOW, *ibid.* **61** (1978) 369.
8. R. MORENA, P. E. LOCKWOOD, A. L. EVANS and C. W. FAIRHURST, *ibid.* **69** (1986) C75.
9. M. A. McCOY and A. H. HEUER, *ibid.* **71** (1988) 673.
10. D. R. CLARKE and B. SCHWARTZ, *J. Mater. Res.* **2** (1987) 801.
11. I. WADSWORTH, J. WANG and R. STEVENS, in "Engineering Ceramics", edited by G. de With, R. A. Terpstra and R. Metselaar (Elsevier Applied Science, London and New York, 1989) p. 3160.
12. N. A. TRAVITZKY and N. CLAUSSEN, in "Advanced Ceramics II", edited by S. Somiya (Elsevier Applied Science, London and New York, 1988) p. 121.
13. D. B. MARSHALL, B. R. LAWN and A. G. EVANS, *J. Amer. Ceram. Soc.* **65** (1982) 561.
14. F. F. LANGE, T. YAMAGUCHI, B. I. DAVIS and P. E. D. MORGAN, *ibid.* **71** (1988) 446.
15. Y. CHENG and D. P. THOMPSON, *Proc. Br. Ceram. Soc.* (1989) 42.
16. J. SELSING, *J. Amer. Ceram. Soc.* **44** (1961) 419.
17. R. W. DAVIDGE and T. J. GREEN, *J. Mater. Sci.* **3** (1968) 629.
18. A. G. EVANS, A. H. HEUER and D. L. PORTER, in Proceedings of 4th International Conference on Fracture **1** (1977) p. 529.
19. R. L. FULLMAN, *Trans. AIME* **196** (1953) 447.
20. B. R. LAWN and T. R. WILSHAW, in "Fracture of Brittle Solids" (Cambridge University Press, Cambridge, 1975).
21. H. RUF and A. G. EVANS, *J. Amer. Ceram. Soc.* **66** (1983) 328.
22. K. T. FABER and A. G. EVANS, *Acta Metall.* **31** (1983) 565.

Received 20 September 1990
and accepted 7 March 1991